

# First-principles Study of Electronic and Dielectric Properties of $\text{ZrO}_2$ and $\text{HfO}_2$

Xinyuan Zhao and David Vanderbilt  
Department of Physics and Astronomy,  
Rutgers University,  
Piscataway, NJ 08854-8019

## ABSTRACT

Using density-functional theory with ultrasoft pseudopotentials, we previously investigated the structural and electronic properties of the low-pressure (cubic, tetragonal, and monoclinic) phases of  $\text{ZrO}_2$  and  $\text{HfO}_2$ , in order to elucidate phonon modes, Born effective charge tensors, and especially the lattice dielectric response in these phases. We now extend this previous work by carrying out similar calculations on the two high-pressure orthorhombic phases, and by providing density-of-states and band-gap information on all polymorphs. Our results show that the electronic structures and dielectric responses are strongly phase-dependent. In particular, the monoclinic phases of  $\text{ZrO}_2$  and  $\text{HfO}_2$  are found to have a strongly anisotropic dielectric tensor and a rather small orientational average ( $\bar{\epsilon}_0$ ) compared to the two other low-pressure phases. Our calculations show that  $\bar{\epsilon}_0$  is even smaller in the orthorhombic phases.

## INTRODUCTION

Dielectrics comprise a class of materials of great technical importance. The most widely-used dielectric in electronics is probably  $\text{SiO}_2$ , which has been persistently exploited in the computer industry for decades due to the excellent quality of the Si/ $\text{SiO}_2$  interface. The dimensions of the gate-dielectric layer (currently  $\text{SiO}_2$ ) have been rapidly reduced to the nanometer scale in order to enhance the speed of CMOS-related devices. Such reductions, however, have uncovered severe fundamental problems that imposed a physical limit on the use of  $\text{SiO}_2$  films as gate dielectrics in the current Si/ $\text{SiO}_2$  semiconductor technology. A great deal of effort has been directed to finding a way to overcome these limits. One particular direction is to use high- $K$  metal oxides with certain desired properties [1] to replace  $\text{SiO}_2$  as the gate dielectric, since the higher dielectric constants of the oxides will allow one to make a physically thicker film while at the same time maintaining (or even increasing) the gate capacitance.

$\text{ZrO}_2$ ,  $\text{HfO}_2$  and their structure-modified derivatives (e.g., Zr and Hf silicates) have emerged as important candidates for this purpose because they have much higher dielectric constants than  $\text{SiO}_2$  ( $\sim 20$  compared with 3.5 for  $\text{SiO}_2$ ) and because of their thermodynamic stability in contact with Si. Experiments have demonstrated their promise for this purpose (see Ref. [1] for a general review). It would be very desirable, therefore, to conduct a systematic theoretical study of the structural, electronic, and dielectric properties of  $\text{ZrO}_2$  and  $\text{HfO}_2$ , and of the dependence of these properties on the choice of crystalline polymorphs or possible modified structures. In two previous works, we studied

the structural and vibrational properties of the three low-pressure phases (cubic, tetragonal, and monoclinic) of  $\text{ZrO}_2$  [3] and  $\text{HfO}_2$  [4], especially the zone-centered phonon modes and the related dielectric properties. These previous works are extended here in two ways. First, we provide density-of-states (DOS) information on all polymorphs of  $\text{ZrO}_2$  and  $\text{HfO}_2$ , which may be helpful in the interpretations of experiments on these materials. Second, we extend our previous calculations of dielectric properties to include the high-pressure orthorhombic phases using the ABINIT package [4]. We have also been engaged in simulating amorphous  $\text{ZrO}_2$  (*a-ZrO}\_2*) using *ab-initio* molecular dynamics as implemented in the VASP [5] package, in a “melt-and-quench” fashion. The resulting amorphous  $\text{ZrO}_2$  structures were analyzed in order to understand their local bonding geometry and other structural properties, and then used as inputs for a first-principles investigation of the vibrational and dielectric properties of the amorphous  $\text{ZrO}_2$  systems using ABINIT. The results will be reported elsewhere.

## CRYSTAL STRUCTURES

$\text{ZrO}_2$  (zirconia) is surprising similar to  $\text{HfO}_2$  (hafnia) in many physical and chemical properties. It is well established that both oxides exhibit three crystalline phases at ambient pressure, i.e., monoclinic, tetragonal and cubic, as temperature is increased. With increasing pressure, phase transitions involving two orthorhombic phases have been reported, although the exact structures of these high-pressure phases has not been established unambiguously ([6,7], and references therein). The first orthorhombic structure used in our simulation (conventionally labeled as Ortho-I) has space group  $Pbca$ ; the other orthorhombic phase (Ortho-II) has space group  $Pnma$ . We study these phases at zero pressure, where they are apparently metastable.

The cubic phase has the fluorite ( $\text{CaF}_2$ ) structure, with 3 atoms (one chemical formula) per primitive unit cell. The tetragonal structure is a slight distortion of the cubic phase obtained by shifting alternating pairs of oxygen atoms up and down along  $\hat{z}$ , and the number of atoms per primitive cell is doubled. The monoclinic phase, which has 12 atoms (four formulas units) per primitive cell, has a more complex structure and lower symmetry. In our calculations of the DOS functions, a 12-atom cell has been used for all of these phases, as in Refs. [2] and [3], in order to facilitate comparison. The monoclinic phase has two non-equivalent oxygen atoms, which evidently will have different site-projected DOS functions. Among the eight oxygens in the unit cell, four are threefold coordinated (denoted as  $\text{O}_1$ ), while the other four (labeled as  $\text{O}_2$ ) are fourfold coordinated. Each threefold oxygen is bonded to three nearest-neighbor metal atoms in an almost planar configuration, while each four-fold oxygen forms a distorted tetrahedron with its four nearest metal neighbors. For the cubic and tetragonal phases, all oxygen atoms are equivalent, although we still use the notation  $\text{O}_1$  and  $\text{O}_2$  for convenience. Detailed discussion of the structures of these phases can be found in Refs. [2] and [3].

A primitive unit cell of the Ortho-I phase (for both  $\text{ZrO}_2$  and  $\text{HfO}_2$ ) consists of 24 atoms, while the Ortho-II phase has 12 atoms per unit cell. We used the lattice parameters given in [6] (Table III there) and [7] (Tables II and III there) as the starting point for our

Table I: Structural parameters calculated for the orthorhombic phases of  $\text{ZrO}_2$  and  $\text{HfO}_2$ . Lattice constants  $a$ ,  $b$  and  $c$ , in Å are given in the first row. Triplets of coordinates indicate the Wyckoff positions of the various atoms.

Phase	$\text{ZrO}_2$	$\text{HfO}_2$
Ortho-I	$a=9.958, b=5.224, c=5.006$	$a=9.837, b=5.129, c=4.954$
	Zr (0.885, 0.035, 0.254)	Hf (0.885, 0.035, 0.254)
	O <sub>1</sub> (0.792, 0.379, 0.133)	O <sub>1</sub> (0.791, 0.376, 0.128)
	O <sub>2</sub> (0.976, 0.739, 0.497)	O <sub>2</sub> (0.977, 0.739, 0.497)
Ortho-II	$a=6.438, b=5.521, c=3.273$	$a=6.353, b=5.435, c=3.240$
	Zr (0.884, 0.256, 0.250)	Hf (0.885, 0.256, 0.250)
	O <sub>1</sub> (0.164, 0.027, 0.250)	O <sub>1</sub> (0.163, 0.025, 0.250)
	O <sub>2</sub> (0.572, 0.142, 0.250)	O <sub>2</sub> (0.573, 0.141, 0.250)

ground-state calculations for Ortho-I and Ortho-II, respectively. The Wyckoff coordinates define two non-equivalent sets of oxygen atoms, labeled by O<sub>1</sub> and O<sub>2</sub>.

## THEORETICAL METHODOLOGY

The DOS functions are computed using a plane-wave implementation of density functional theory (DFT) in the local-density approximation (LDA) as parametrized by Ceperley and Alder [8], using ultra-soft pseudopotentials [9]. Although a  $4 \times 4 \times 4$   $\mathbf{k}$ -point sampling was found to provide sufficient precision in calculating total energies and forces, we used a refined mesh of  $\mathbf{k}$ -points and higher 36-Ry cut-off to obtain smoother and more accurate DOS functions. The  $\mathbf{k}$ -point meshes used in the DOS calculations are  $20 \times 20 \times 20$  for cubic and tetragonal,  $10 \times 10 \times 10$  for monoclinic,  $12 \times 12 \times 12$  for Ortho-I, and  $16 \times 16 \times 16$  for Ortho-II phases. In calculating the site-projected partial DOS, spherical radii of 0.9 Å and 1.25 Å are used for the metal ions (Zr or Hf) and oxygen ions respectively. For cubic and tetragonal phases, the larger 12-atom unit cell was used in the calculations, so the DOS values should be reduced accordingly if the DOS per primitive cell is desired. Further details can be found in [2] and [3].

The dielectric response of orthorhombic phases of  $\text{ZrO}_2$  was calculated by specialized linear-response techniques as implemented in ABINIT [4], taking into account the coupling between phonons and the homogeneous electric field. A  $4 \times 4 \times 4$   $\mathbf{k}$ -point mesh, Troullier-Matins type pseudopotentials [10] (4 and 6 valence electrons for Zr and O respectively), and an energy cutoff of 35.0 Hartree provide satisfactory convergence.

## RESULTS

In Table I we present our calculated lattice parameters for the two orthorhombic phases, which agree well with the previous theoretical calculations [6,7]. Because the computed DOS functions for  $\text{HfO}_2$  and  $\text{ZrO}_2$  are so similar, we only present those for  $\text{HfO}_2$  here, shown in Figs. (1)-(3). Some comparisons are given later in Table II for both oxides.

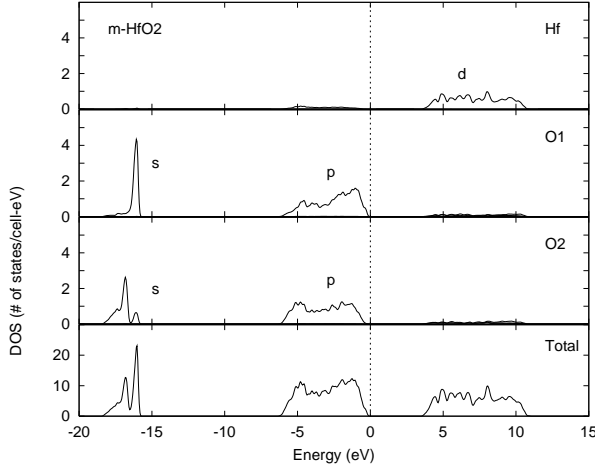


Figure 1: Density of states (DOS) for monoclinic  $\text{HfO}_2$ . Upper panels show the orbital-projected partial DOS for Hf,  $\text{O}_1$ , and  $\text{O}_2$ , respectively. Lower panel shows the total DOS. Vertical dashed line indicates the valence-band maximum.

Figure 1 shows the total DOS (lowest panel) and the site-projected partial DOS (upper three panels) for monoclinic  $\text{HfO}_2$ . We find this material to be an insulator with a band gap of 3.5 eV, in good agreement with previous theoretical results (3.48 eV in [11] and 3.6 eV in [12]). The bands in the energy range from  $-20$  eV to  $-15$  eV are mostly due to  $\text{O } 2s$  orbitals. The next bands, spanning between  $-6$  eV and 0, are mainly  $\text{O } 2p$  in character, and Hf  $5d$  orbitals dominate the unoccupied conduction bands ranging from 3 eV up to 11 eV. The two non-equivalent oxygen sites have noticeably different DOS features, as expected from their different surroundings.

In Fig. 2, we provide the DOS functions calculated for cubic and tetragonal  $\text{HfO}_2$ . It can be readily seen that these two phases have rather similar DOS features. Cubic  $\text{HfO}_2$  has a band gap of 3.2 eV, while for tetragonal  $\text{HfO}_2$  it is 3.8 eV. Ref. [11] gives 3.4 eV and

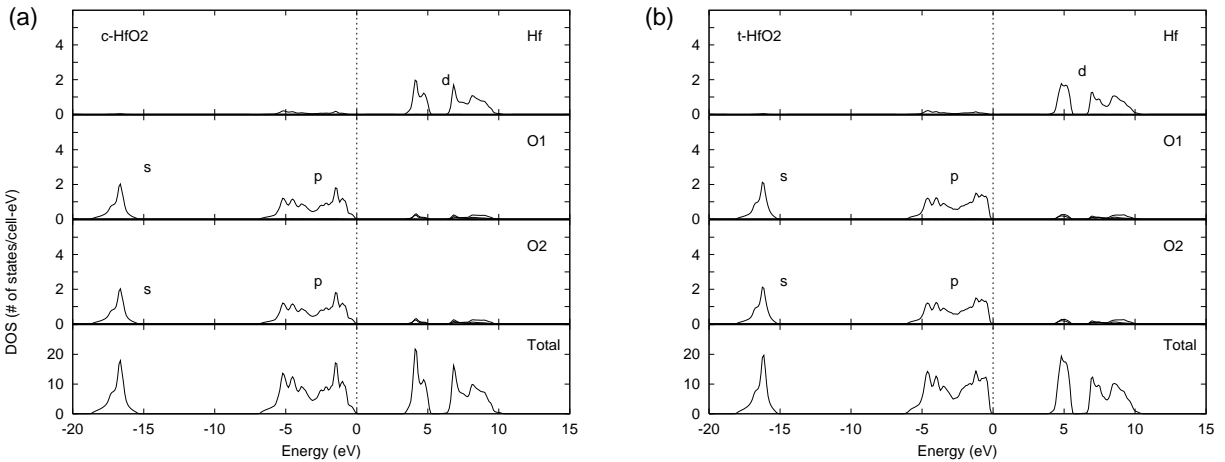


Figure 2: Same as in Fig. 1, but now for cubic (a) and tetragonal (b) phases of  $\text{HfO}_2$ .

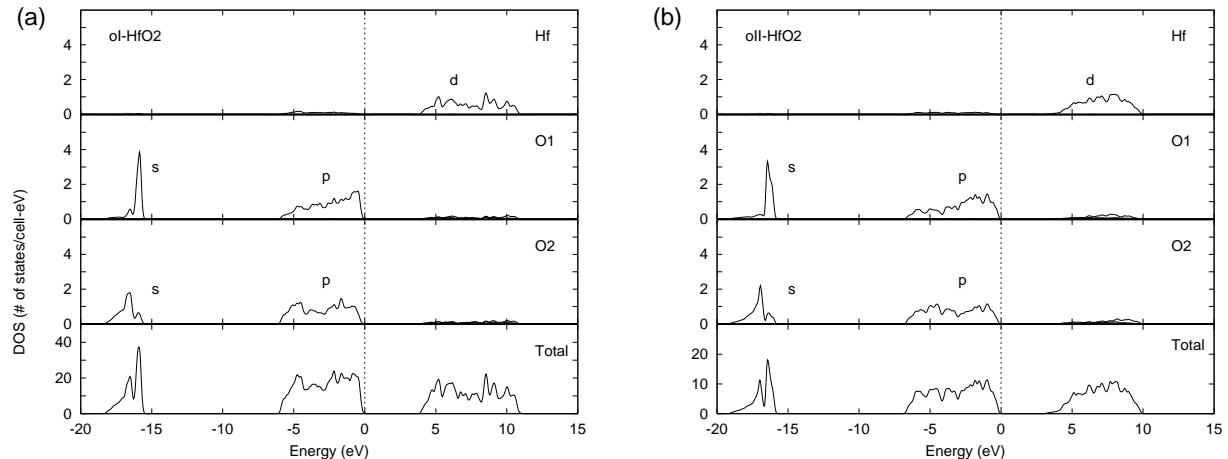


Figure 3: Same as Fig. 1, but now for the two orthorhombic phases of  $\text{HfO}_2$ .

3.77 eV for the cubic and tetragonal phases, respectively. Again, both theoretical works agree quite well. The most significant difference between these two phases and the monoclinic phase is that the Hf  $d$ -like states separate into two bands in the cubic and tetragonal phases, but form a single band in the monoclinic phase. The DOS functions for the two high-pressure orthorhombic phases are presented in Fig. 3, from which one readily sees that the oxygen atoms exhibit two quite different types of DOS, as in the monoclinic phase. In fact, there is a surprising degree of resemblance of the monoclinic DOS with that of the Ortho-I and Ortho-II phases, especially the former.

The DOS functions of the  $\text{ZrO}_2$  polymorphs (not shown) are qualitatively very similar to the corresponding ones for  $\text{HfO}_2$ . The most important differences are in the band gaps. Because of LDA error, the absolute values of the band gaps are not reliable, but trends should be meaningful. As shown in Table II, we find that the band gaps are systematically larger (by  $\sim 0.5$  eV) for  $\text{HfO}_2$  than for  $\text{ZrO}_2$ , and that variations of crystal structure can lead to band gap changes of order 1 eV. Also tabulated in Table II are our calculated dielectric constants (orientational average  $\bar{\epsilon}_0$ ) for  $\text{ZrO}_2$  and  $\text{HfO}_2$  polymorphs. For the low-pressure cubic, tetragonal, and monoclinic phases, the dielectric constants are quoted from [2] and [3], where the full dielectric tensors are given. For the Ortho-I and II phases of  $\text{ZrO}_2$ , the linear-response scheme [4] is utilized in the calculation of the static dielectric tensors, which includes the lattice contributions as well as the electronic screening. In orthorhombic  $\text{ZrO}_2$ ,  $\bar{\epsilon}_0$  becomes even smaller, approximately 20 and 18 for the Ortho-I and II phases, respectively. The dielectric tensors for the orthogrombic phases are diagonal, with elements (22.6, 18.1, 19.6) and (18.8, 18.9, and 17.8) for Ortho-I and Ortho-II respectively. The average principal values of the Born effective charge tensors are about 5.0 and 2.5 for Zr and O atoms respectively for both orthorhombic phases.

## CONCLUSIONS

We studied the structural, electronic, vibrational and dielectric properties for nearly

Table II: Band gaps ( $E_g$ ) and orientationally averaged dielectric constants ( $\bar{\epsilon}_0$ ) calculated for crystalline phases of  $\text{ZrO}_2$  and  $\text{HfO}_2$ .  $E_g$  values in parentheses for  $\text{HfO}_2$  are from the theory of Ref. [11].

Phase	$\text{ZrO}_2$		$\text{HfO}_2$	
	$E_g$ (eV)	$\bar{\epsilon}_0$	$E_g$ (eV)	$\bar{\epsilon}_0$
Cubic	2.63	37	3.15 (3.40)	29
Tetragonal	3.31	38	3.84 (3.77)	70
Monoclinic	2.98	20	3.45 (3.48)	16–18
Ortho-I	3.06	20.1	3.75	-
Ortho-II	2.29	18.5	2.94	-

all the currently well-recognized phases of  $\text{ZrO}_2$  and  $\text{HfO}_2$ , using advanced first-principles techniques, with a special focus on the dielectric properties. It is found that the crystalline structure can have a substantial effect on the band gaps and dielectric constants. Our results show that the dielectric response depends strongly on the crystal phase, and can span a wide range of values ( $\bar{\epsilon}_0 = 18 - 40$  for  $\text{ZrO}_2$ ). Monoclinic  $\text{ZrO}_2$  (or  $\text{HfO}_2$ ) has a rather anisotropic dielectric tensor and a smaller averaged dielectric constant than the tetragonal and cubic phase. The  $\bar{\epsilon}_0$  of the Ortho-I and II phases appear even smaller. We hope that these theoretical results will shed light on the potential for  $\text{ZrO}_2$ ,  $\text{HfO}_2$  or their derivatives to replace  $\text{SiO}_2$  as the gate dielectric in CMOS technology, and will provide hints for manipulating these oxides to serve this purpose.

## ACKNOWLEDGMENTS

This work has been supported by NSF Grant DMR-9981193. We wish to thank E. Garfunkel and S. Sayan for useful discussions. One of authors (X.Z.) thanks G.-M. Rignanese for assistance with ABINIT.

## REFERENCES

1. G. D. Wilk, R. M. Wallace, and J. M. Anthony, *J. Appl. Phys.* **89**, 5243 (2001).
2. X. Zhao and D. Vanderbilt, *Phys. Rev. B* **65**, 75105 (2002).
3. X. Zhao and D. Vanderbilt, *Phys. Rev. B* **65** 233106 (2002).
4. X. Gonze et al., *Mater. Sci.* **25**, 478 (2002).
5. G. Kresse and J. Hafner, *Phys. Rev. B* **47**, R558 (1993); **54**, 11169 (1996).
6. J. K. Dewhurst and J. E. Lowther, *Phys. Rev. B* **57**, 741 (1998).
7. G. Jomard, T. Petit, A. Pasturel, L. Magaud, G. Kresse, and J. Hafner, *Phys. Rev. B* **59**, 4044 (1999).
8. D. M. Ceperley and B. J. Alder, *Phys. Rev. Lett.* **45**, 566 (1980).
9. D. Vanderbilt, *Phys. Rev B* **41**, 7892 (1990).
10. N. Troullier and J. L. Martins, *Phys. Rev. B* **43**, 1993 (1991).
11. A. A. Demkov, *Phys. Stat. Sol. B* **226**, 57 (2001).
12. P. K. Boer and R. A. de Groot, *J. Phys.: Condens. Matter* **10**, 10241 (1998).